New impact picture for low- and high-energy proton-proton elastic scattering

C. Bourrely and J. Soffer

*Centre de Phsique Théorique, Centre National de la Recherche Scientifique, Marseille, France**

Tai Tsun Wu[†]

Instituut voor Theoretische Fysica, Rijksuniversiteit, Utrecht, The Netherlands

(Received 24 May 1978)

We improve significantly the impact picture that was used several years ago to predict the increase of total and integrated differential cross sections at high energies. The major improvements consist of the following: (1) The dependence of the Pomeron term on the momentum transfer is taken from a modified version of the relation between matter distribution and charge distribution, (2) Regge backgrounds are properly taken into account, and (3) a simple nontrivial form is used for the hadronic-matter current in the proton. For proton-proton elastic scattering, the phenomenological differential cross section is in good agreement with the experimental data in the laboratory momentum range of 14 to 2000 GeV/c, and is predicted for ISABELLE energy. Because of the third improvement, predictions are obtained for both polarization and R parameters for proton-proton elastic scattering.

I. INTRODUCTION

In order to have some theoretical understanding of scattering processes at extremely high energies, one useful approach is to study the high-energy behavior of quantum field theory. In any relativistic quantum field theory, many fundamental properties of the S matrix are automatically satisfied, including in particular the presence of production processes, s-channel unitarity, t-channel unitarity, analyticity, and crossing symmetry. For this reason, in relativistic quantum field theory we have a theoretical laboratory to investigate the interrelation of these general properties together with their implications on high-energy processes.

A first result of such an investigation[1] is that the Froissart bound[2] is not merely an upper bound but is actually saturated. In other words, in the high-energy limit $s \to \infty$, the total cross section increases as $(\ln s)^2$, where s is the square of the center-of-mass energy. Three years later, increasing cross section was found experimentally at CERN ISR for proton-proton scattering,[3] although we cannot conclude in the presently available energy range that the Froissart bound is actually saturated. By now, there is a great deal of experimental information on this subject from both ISR and Fermilab. It is the purpose of this paper to carry out a phenomenological analysis of these data on proton-proton scattering in a way compatible with the results of quantum field theory.

Several years ago, when there was as yet very little experimental information, such a phenomenological analysis, referred to as an impact picture, was carried out.[4] This earlier analysis was successful in giving a number of predictions that were verified later, such as the increase of the πp and Kp total cross sections, and the large ratio of Kp to pp differential cross sections. However, this earlier analysis (see for a more recent summary Ref. 5) also has a number of major defects; the present work contains the following significant improvements:

(i) In the dependence on momentum transfer, the form of the Pomeron term is taken from a modified version of the relation between matter distribution and charge distribution.[6,7] In the earlier analysis,[4] because of the absence of data, this form was chosen arbitrarily for computational convenience.

(ii) In the dependence on energy, Regge background terms are properly included. In the earlier analysis, these terms are taken into account only in the forward direction.

(iii) The spin dependence of the proton in the Pomeron term is constructed within a simple physical picture of rotation of matter inside the proton. This construction is based on the concept of hadronic current density of Chou and Yang.[8] It is thus possible to study the polarization and rotation parameters.

On the other hand, a number of the simplifying assumptions used previously[4] are still retained. They include in particular the following two:

(1) The contribution to opaqueness due to the Pomeron is assumed to be factorized into the product of a function of energy and one of the impact parameter [see (2) below]. This factorization is sometimes referred to as geometrical scaling.

(2) The opaqueness for any fixed impact parameter is assumed to increase without bound in the limit of infinite energy.

It must be realized that neither of these assumptions has support from quantum field theory,[1] and almost certainly requires modification in the future. In particular, the second assumption means that we use the factor $1 - e^{-\Omega(s,\vec{b})}$ below in (1) while it should more generally be $\alpha[1 - e^{-\Omega(s,\vec{b})}]$ with $\alpha \lesssim 1$. This assumption has been extensively discussed before [see Sec. 4(H) of Ref. 4], and the presence of $\alpha < 1$ means, on the basis of quantum field theory, the most interesting possibility of the existence of hadronic states that couple very weakly to the Pomeron.

The present phenomenological analysis covers the range in laboratory momentum from 14 to 2000 GeV/c. Special attention is given to the absence of the second dip in pp differential cross section. Predictions for energies of future accelerators such as ISABELLE are presented.

II. DESCRIPTION OF THE MODEL

In this section we describe our model in view of an analysis of the experimental data on total and differential cross sections. In the impact parameter representation we write the proton-proton elastic amplitude as

$$M(s,t) = \frac{is}{2\pi} \int e^{-i\vec{q}\cdot\vec{b}} (1 - e^{-\Omega(s,\vec{b})})d\vec{b} , \qquad (1)$$

where $\vec{q}$ is the momentum transfer, $t = -\vec{q}^2$ and $\Omega(s,\vec{b})$ is defined to be the opaqueness at the impact parameter $\vec{b}$ which is also a function of the energy $\sqrt{s}$. The colliding particles carry a spin $\frac{1}{2}$ and as a result $\Omega(s,\vec{b})$ is a spin-dependent function. The spin dependence of Ω will be treated in Sec. IV, and for the moment let us define $\Omega_0(s,\vec{b})$ corresponding to the spin-independent part of the amplitude as a sum of two terms

$$\Omega_0(s,\vec{b}) = S_0(s)F(\vec{b}^2) + R_0(s,\vec{b}) . \qquad (2)$$

The first term associated to the "Pomeron" exchange, is responsible for the diffractive component, and the second term is a Regge background whose contribution is needed to describe the low-energy data. For the diffractive term a simple choice is to assume[4] that the s and the $\vec{b}$ dependence factorize such that we have a product of two functions $S_0(s)$ and $F(\vec{b}^2)$. The expression for $S_0(s)$ is taken from the high-energy behavior of quantum field theory[1] and we shall use the crossing-symmetric expression[4]

$$S_0(s) = \frac{s^c}{(\ln s)^{c'}} + \frac{u^c}{(\ln u)^{c'}} , \qquad (3)$$

where u is the third Mandelstam variable. Note that $S_0(s)$ is complex.

The impact-parameter dependence of the Pomeron is contained in $F(\vec{b}^2)$ for which various ansatz have been proposed that we want to discuss briefly. In the earlier analysis[4] $F(\vec{b}^2)$ was chosen to be proportional to the function $\exp[-\lambda(b^2 + b_0^2)^{1/2}]$. For such a function the calculated amplitude has the interesting feature that it gives *one dip* in the differential cross section (once the parameters are adjusted), but it suffers from a fast decrease at large t, and it is below the recent ISR data by a few orders of magnitude. Another ansatz follows from the proportionality between the charge density of the proton and the internal distribution of matter.[6,7] If this proportionality is assumed to be exact, and a multipole approximation is used for the electromagnetic form factor of the proton, then the resulting amplitude gives a fair description of the differential cross section at ISR energies up to 2 GeV^2, but gives also around $|t| \sim 4$ GeV^2 a second dip, which is not observed at ISR.

Here we present a solution which overcomes the difficulties mentioned above by supposing that $\tilde{F}(t)$ is not only proportional to the square of the form factor, but also proportional to a slowly varying function of t which has a real zero. This possibility is not ruled out by quantum field theory, since the relation between $\tilde{F}(t)$ and the electromagnetic form factor is not exact.[9] We shall take

$$\tilde{F}(t) = f [G(t)]^2 \frac{a^2 + t}{a^2 - t} , \qquad (4)$$

with

$$G(t) = \frac{1}{(1 - t/m_1^2)(1 - t/m_2^2)} . \qquad (5)$$

The term $G(t)$ corresponds to a reasonable parametrization of the form factor, while the last factor in (4) represents an approximation to the remaining t dependence which is unknown at present. More elaborate expressions can be used provided they give a zero at a similar t value, but the function we propose involves only one free parameter and is a very simple one. Let us stress that with the slowly varying function introduced in Eq. (4) factorization is violated since it cannot be expressed as a product of vertex functions unless new branch cut singularities occur. However, our Pomeron is a fixed cut so we do not need to preserve factorization.

Since we are interested in the analysis of low-energy data, we must add a spin-independent Regge background that we shall take as

$$\tilde{R}_0(s,t) = [C_+ + C_- e^{-i\pi\alpha(t)}]s^{\alpha(t)} , \qquad (6)$$

representing the standard even- and odd-signature exchange contributions, with an exchange-degenerate trajectory $\alpha(t) = \alpha_0 + \alpha' t$. Notice that in
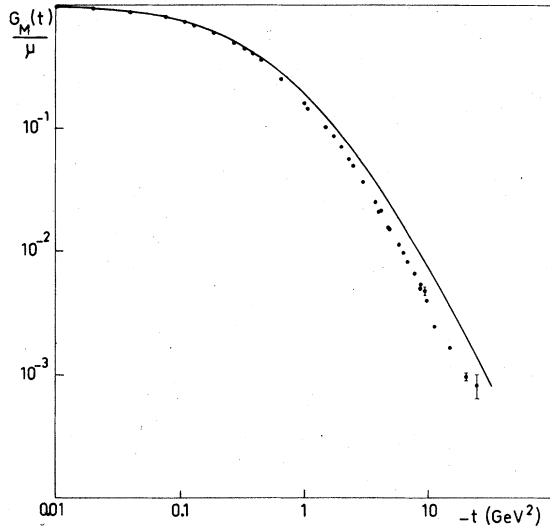
FIG. 1. Proton electromagnetic form factor $G_M(t)/\mu$ compared with the function $G(t)$ given by Eq. (5) (solid curve). For a compilation of the data see Ref. 10.

Ref. 4 only the energy dependence of σ_{tot} was fitted so a simple term as $A/\sqrt{s}$ was used instead of this Regge contribution.

Summarizing all the above expressions Eqs. (3)–(6), we get

$$\tilde{\Omega}_0(s,t) = S_0(s)\tilde{F}(t) + \tilde{R}_0(s,t) , \tag{7}$$

whose Fourier transform provides $\Omega_0(s,b)$ from which one can calculate the spin-independent amplitude

$$a_0(s,t) = is \int_0^\infty J_0(b\sqrt{-t})(1 - e^{-\Omega_0(s,b)})b\,db . \tag{8}$$

III. NUMERICAL RESULTS

The amplitude a_0 involves ten parameters that we fitted by taking the $\bar{p}p$ total-cross-section data and the elastic pp data on σ_{tot}, $\rho = \mathrm{Re}a_0/\mathrm{Im}a_0$, and $d\sigma/dt$ in the momentum range from 14 GeV/c up to 2000 GeV/c. As a result of the fit we have obtained the following values:

$$c = 0.151, \quad c' = 0.756 ,$$

$$m_1 = 0.619 \text{ GeV}, \quad m_2 = 1.587 \text{ GeV},$$

$$a = 2.257 \text{ GeV}, \quad f = 8.125, \tag{9}$$

$$C_+ = -39, \quad C_- = 1.8 ,$$

$$\alpha(t) = 0.352 + 0.694t ,$$

with t in units of (GeV)^2. The asymptotic energy regime of hadronic interactions is controlled by c and c' and the above values obtained by using a very large set of data are more accurate than those from the previous determination.[4]

A comparison of the model with experimental data is displayed in Figs. 1-9, and let us now discuss the results in some details. The double-pole term $G(t)$ in Eq. (5) can be interpreted as the "form factor." In Fig. 1, $G(t)$ is plotted versus $-t$ with the values of m_1 and m_2 fitted from the differential cross section, the curve has the correct shape compared with the experimental electromagnetic form factor,[10] however, for large t it lies above the data points. Since we do not expect an exact connection with the form factor,[9] we consider that this double-pole parametrization is an approximate fit to the form factor.

The profile functions are shown in Fig. 2. The curve labeled $\Omega_G(b)$ represents the Fourier transform of $f[G(t)]^2$, and we observe that the introduction of a zero in Eq. (4) flattens the curve $F(\tilde{b}^2)$ in the low-b region. Such a difference is necessary to reproduce correctly the large-t behavior of the cross section. A similar flattening effect has been obtained in a model of the quark-gluon structure of the proton by Van Hove,[15] who assumes that the gluon amplitude is close to the unitarity limit at small impact parameter distance.

The total cross sections σ_{tot} and the ratio $\rho = \mathrm{Re}a_0/\mathrm{Im}a_0$ are presented in Figs. 3, 4 as a check of the forward values of the amplitude. The Figs. 5–8 show the fair agreement of the model with the differential cross section between 14 and 2000 GeV/c, in particular at $p_{lab} = 1480$ GeV/c (see Fig. 7) we get the correct slope of the cross section up to $|t| = 10$ GeV^2 and no second dip arises at such energy. We have also checked the energy dependence at fixed t ($-t = 6$ GeV^2) in Fig. 9. The curve reproduces the general trend of the data, and we predict that the cross section is decreasing slowly with energy above $\sqrt{s} = 70$ GeV. For $\sqrt{s} < 25$ GeV where the Regge background is important, we observe that the theoretical curve lies below the data. This means that, for large $|t|$ around 6 GeV^2, the simple Regge contribution that we have used decreases too rapidly. As a possible further test of this Regge background, we plan in the future to calculate from the present phenomenology the case of antiproton-proton scattering, where no new parameter is needed. Possible significant deviations between the theory and the data may give valuable information about the Regge terms. Finally we remark that our "input" Regge trajectory $\alpha(t) = 0.352 + 0.654t$ is lower and flatter than usual, but after the eikonalization we have checked that we obtain a normal trajectory which gives, for example, the correct crossover t value for pp and $\bar{p}p$ as in Ref. 16.
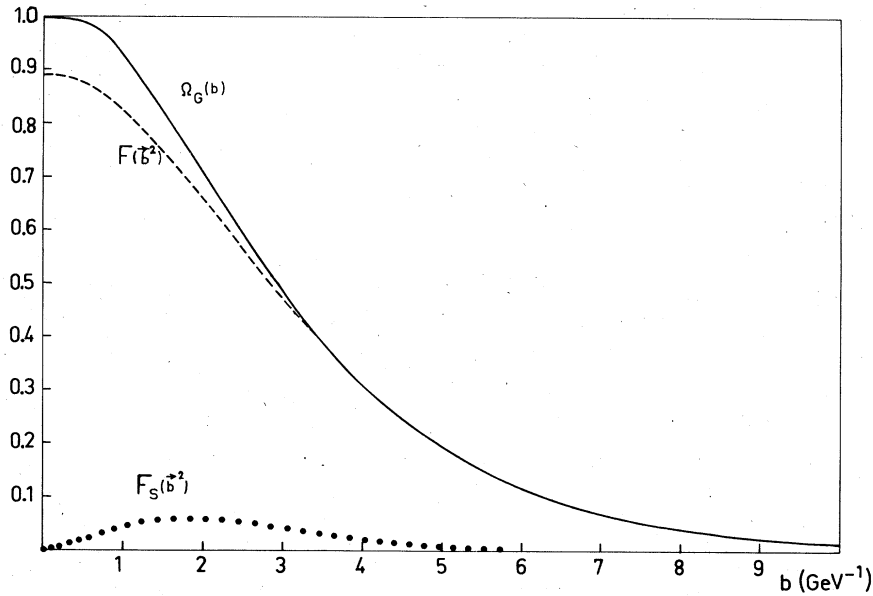
In view of the energy domain accessible to the

FIG. 2. Profile functions. $\Omega_G(b)$ (solid curve) corresponds to the Fourier transform of $f[G(t)]^2$, $F(\vec{b}^2)$ (dashed curve) to the tranform of Eq. (4), and $F_s(\vec{b}^2)$ (dotted curve) is the spin-dependent profile function corresponding to soft rotation.

future accelerators (ISABELLE), Fig. 10 shows predictions at $\sqrt{s} = 200$ and 800 GeV. We note that no second dip appears at these very high energies because $\mathrm{Im}\,a_0(s,t)$ has only one zero. This is certainly different from the approach of Chou and Yang[17] who expect the development of a second dip due to a slowly decreasing real part.

IV. SPIN STRUCTURE OF THE MODEL

Up to now we have ignored the proton spin because the data we have analyzed are not sensitive

to this degree of freedom. In the following we will show that with some simple hypothesis concerning the structure of the proton we are able to construct a spin-dependent amplitude and then to calculate the polarization and the R parameter at different energies.

The concept of matter current inside a hadron is due to Chou and Yang.[8] They study the existence of a hadronic matter current inside a polarized hadron as a complementary aspect of their original hypothesis on hadronic matter
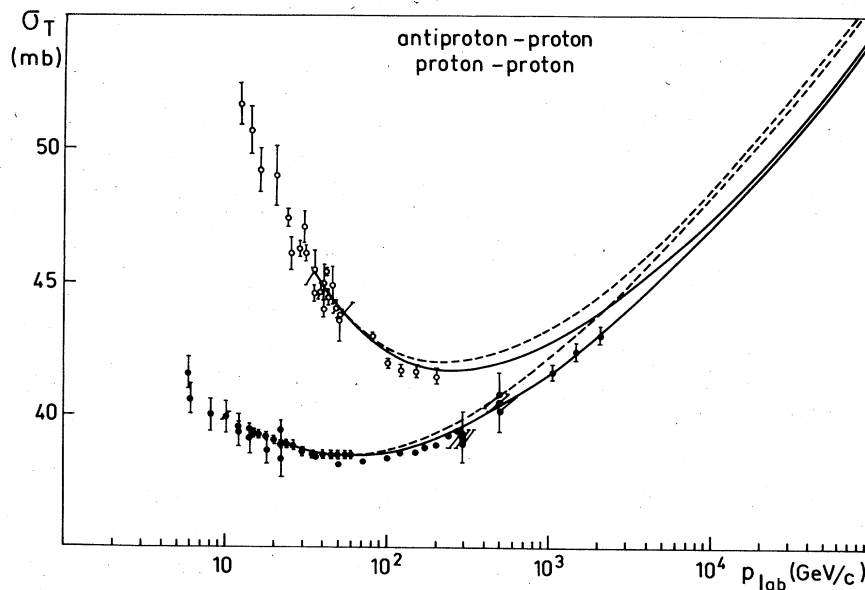
FIG. 3. σ_{tot} proton-proton (black circles) and antiproton-proton (open circles) (data are from Ref. 11), and prediction for ISABELLE energies. The solid curves are our model fit, and the dashed curves are the predictions of Ref. 4 with $c' = 0$.
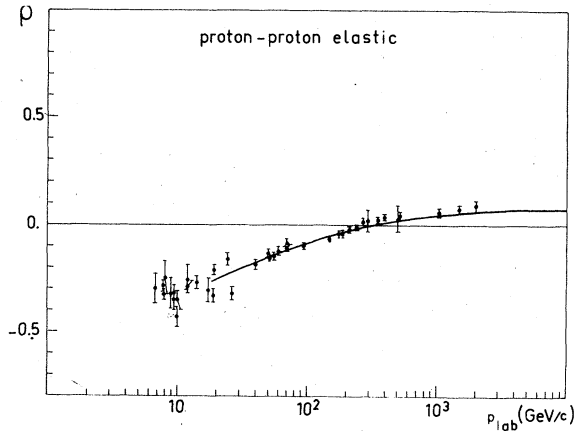
FIG. 4. $\mathrm{Re}a_0/\mathrm{Im}a_0$ as a function of p_{lab} (data from Ref. 12). The curve is our model fit.

density, the two concepts being analogous to the electromagnetic charge and current densities.

As a consequence of their hypothesis, the presence of an hadronic matter current makes the interaction spin dependent and this leads to specific predictions on spin-correlation parameters, in particular, the R parameter.[8]

Let us assume that the scattering of two protons occurs in the x-y plane with the direction of the

incident proton along the y axis. Consider a small region of the target and call v_y the y component of the velocity of this region in the c.m. system of this region and of the projectile. The effective energy of the projectile in the rest-system region of the target is

$$s_{\mathrm{eff}} = s(1 - v_y),\qquad(10)$$

where higher-order terms in v_y have been neglected. From Eq. (3) the energy dependence of the Pomeron exchange becomes now

$$S_0(s) \rightarrow S(s,\vec{b}) = S_0(s_{\mathrm{eff}}) \sim S_0(s) - sv_y\frac{\partial}{\partial s}S_0(s)$$

$$= \frac{s^c}{(\ln s)^{c'}} - sv_y\frac{\partial}{\partial s}\frac{s^c}{(\ln s)^{c'}}$$

$$+ \text{cross terms in } u.\qquad(11)$$

The quantity v_y describes the motion of hadronic matter inside a proton, and is determined in a complicted way by strong interactions. For the present purposes, we propose to proceed with the simplest possible assumptions. In this section, we consider the case of *rigid rotation*

$$v_y = \omega b_x = \omega\hat{b}_x b\qquad(12)$$

where ω is the angular velocity of the rigid rotation, $\hat{b} = \vec{b}/b$ is a unit vector, and $\hat{b}_x$ is the x com-
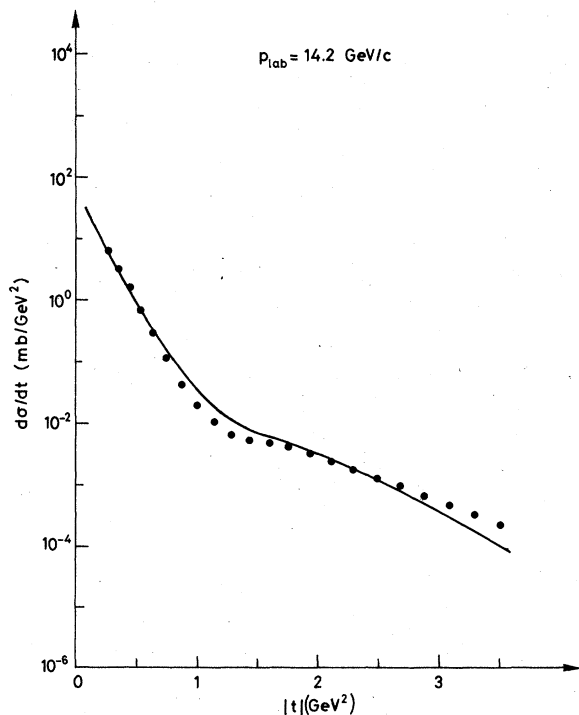

FIG. 5. Proton-proton differential cross section at $p_{\mathrm{lab}} = 14.2$ GeV/c (data from Ref. 13). The curve is our model fit.
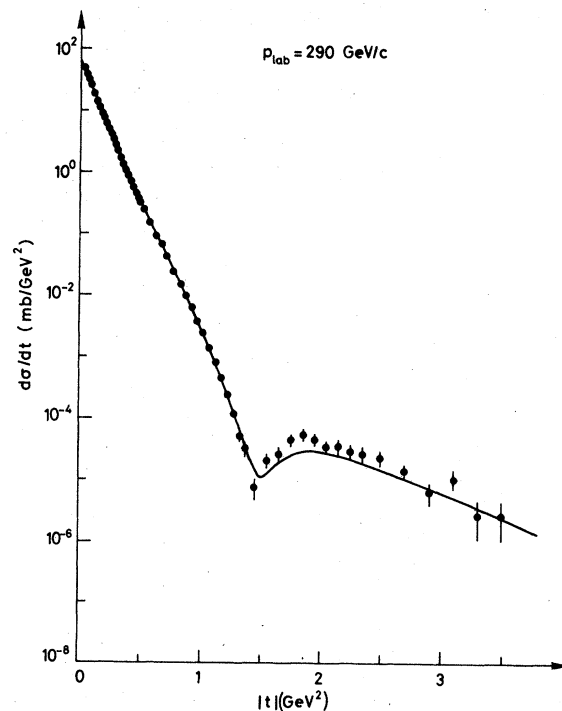

FIG. 6. Proton-proton differential cross section at $p_{\mathrm{lab}} = 290$ GeV/c (data from Ref. 14). The curve is our model fit.
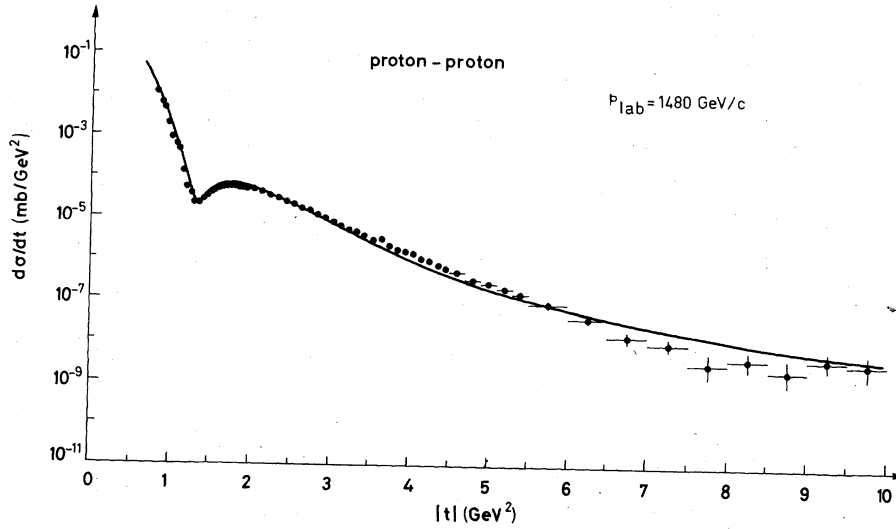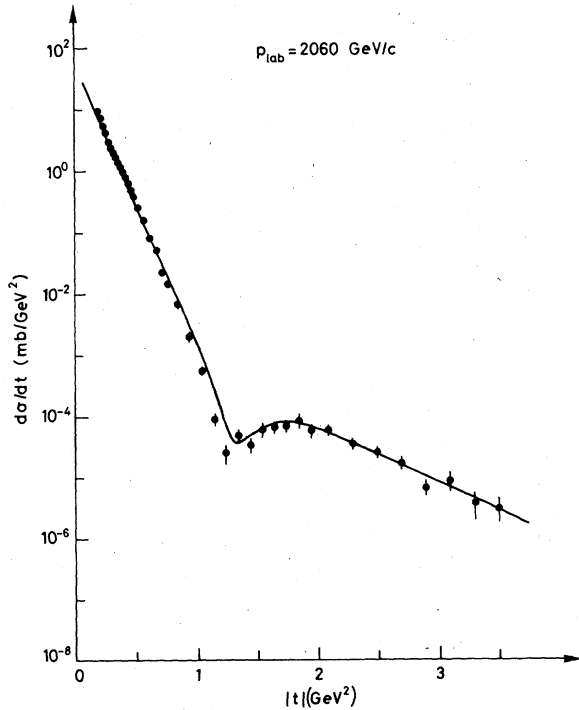
FIG. 7. Proton-proton differential cross section at p_{lab} =1480 GeV/c (data from Ref. 14). The curve is our model fit.

ponent of $\hat{b}$.

Since rigid rotation is specified by only one parameter ω, it is the simplest conceivable assumption, but it clearly has qualitatively undesirable features. Thus in the next section we shall consider a somewhat more complicated form

of v_y.

From (11) and (12) we obtain

$$S(s,\vec{b}) = S_0(s) - \omega\hat{b}_x bS_1(s) ,\qquad(13)$$

where

$$S_1(s) = \frac{s^c}{(\ln s)^{c'}}\left(c - \frac{c'}{\ln s}\right) + \frac{u^c}{(\ln u)^{c'}}\left(c - \frac{c'}{\ln u}\right).$$

The sign of v_y is related to the spin orientation of the target so we have

$$S(s,\vec{b}) = S_0(s) \mp \omega\hat{b}_x bS_1(s) ,\qquad(13')$$

FIG. 8. Proton-proton differential cross section at p_{lab}=2060 GeV/c (data from Ref. 14). The curve is our model fit.
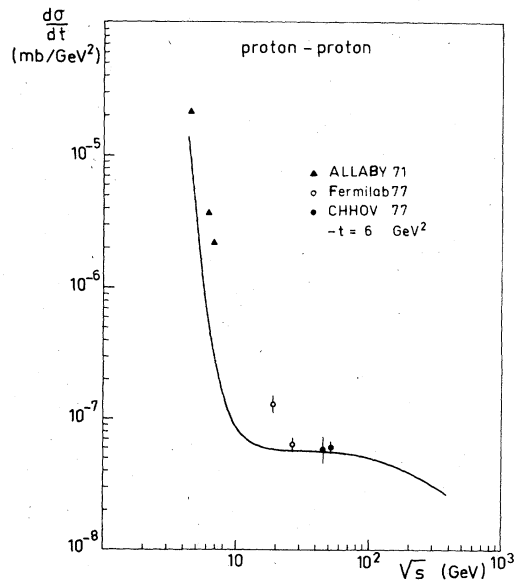

FIG. 9. Proton-proton differential cross section as a function of $\sqrt{s}$ and fixed $-t = 6$ GeV^2 (data from Ref. 13 and 14). The curve is our model prediction.
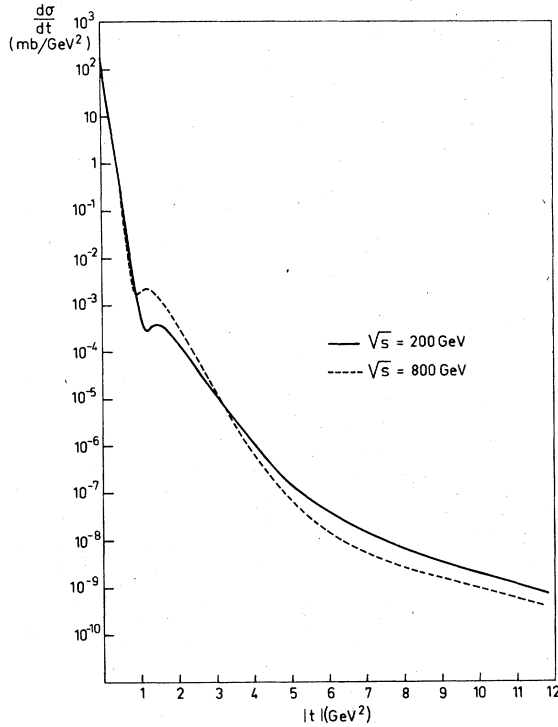
FIG. 10. Proton-proton differential cross section at $\sqrt{s} = 200$ and 800 GeV. The two curves are our model predictions.

where $\mp$ for target spin $\pm\frac{1}{2}$ along the z axis.

We differ from the pioneering work of Chou and Yang[8] in two respects. First, their hadronic matter motion is not described by (12); and secondly, because $S(s,\vec{b})$ as given by (13) is complex, we get a nonvanishing polarization at high energies when the Pomeron dominates.

The total opaqueness $\Omega(s,\vec{b})$ which occurs in Eq. (1) is obtained in this case from Eq. (2) by the substitution $S_0(s) \to S(s,\vec{b})$ given by Eq. (13′) which yields

$$\Omega(s,\vec{b}) = \Omega_0(s,b) \mp \Omega_1(s,b)\hat{b}_x , \qquad (14)$$

with

$$\Omega_1(s,b) = F_s(\vec{b}^2)S_1(s) + R_1(s,b) , \qquad (15)$$

where $F_s(\vec{b}^2) = b\omega F(\vec{b}^2)$ and $R_1(s,b)$ is a necessary Regge spin-dependent contribution in order to study polarization and rotation parameters at low energies. More explicitly, $R_1(s,b)$ is the Fourier transform of the standard Regge background

$$\tilde{R}_1(s,t) = \sqrt{-t}\,[C'_+ + C'_- e^{-i\pi\alpha(t)}]e^{Bt}s^{\alpha(t)} , \qquad (16)$$

which has the appropriate kinematical factor $\sqrt{-t}$ and an exponential damping factor in the residue. This damping factor which should be included in general was not necessary for the spin-independent amplitude $a_0(s,t)$ (see also Ref. 16).

The total scattering amplitude defined by Eq. (1) can be written as

$$M(s,t) = a_0(s,t) + i\,\vec{\sigma}\cdot\vec{n}\,a_1(s,t) , \qquad (17)$$

where $\vec{n}$ is a unit vector normal to the scattering plane, $a_0(s,t)$ is given by Eq. (8), and the spin-dependent amplitude $a_1(s,t)$ reads

$$a_1(s,t) = is \int_0^\infty J_1(b\sqrt{-t})\Omega_1(s,b)e^{-\Omega_0(s,b)}b\,db , \qquad (18)$$

where the Bessel function J_1 comes from the angular integration.

In addition, we have included the real contribution of one-photon exchange to the scattering amplitudes a_0 and a_1 which leads to a sizeable effect in the polarization at high energies and large momentum transfer (see Ref. 18).

Let us finally recall the expressions in terms of the amplitude $a_0(s,t)$ and $a_1(s,t)$ of the four observables in the laboratory system corresponding to the scattering with a polarized proton target. These observables are

$$\sigma_0 = |a_0|^2 + |a_1|^2 , \qquad (19)$$

$$\sigma_0 P = 2\,\mathrm{Im}(a_0 a_1^*) , \qquad (20)$$

$$\sigma_0 R_{1ab} = -(|a_0|^2 - |a_1|^2)\cos(\theta - \theta_R) \\ -2\,\mathrm{Re}(a_0 a_1^*)\sin(\theta - \theta_R) , \qquad (21)$$

$$\sigma_0 A_{1ab} = -(|a_0|^2 - |a_1|^2)\sin(\theta - \theta_R) \\ +2\,\mathrm{Re}(a_0 a_1^*)\cos(\theta - \theta_R) , \qquad (22)$$

where θ is the center-of-mass scattering angle, θ_R is the recoil angle in the laboratory system.

V. SPIN STRUCTURE OF THE MODEL (CONTINUED)

Although rigid rotation involves the least number of parameters, it is unsatisfactory from a
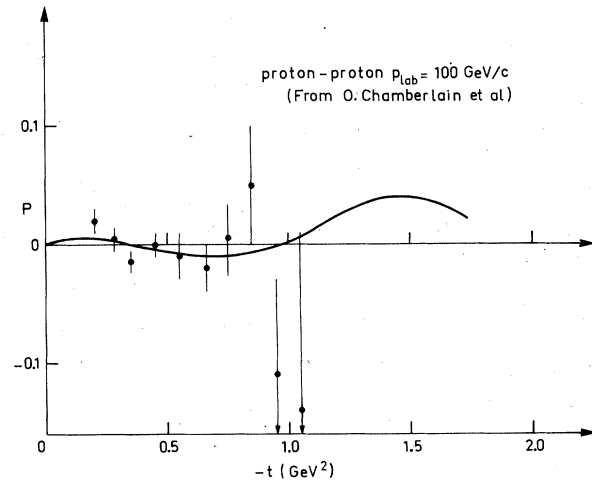

FIG. 11. Polarization at 100 GeV/c (data from Ref. 19). The curve is the fit of our rigid-rotation model.
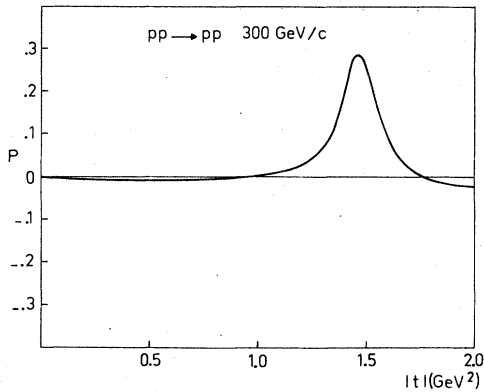
FIG. 12. Prediction of our rigid-rotation model for the polarization at 300 GeV/c.

FIG. 13. Prediction of our rigid-rotation model for R_{lab} at 100, 280, 1480 GeV/c.

theoretical point of view for the following reason. Consider the mathematical limit of $s \to \infty$, where contributions from the large impact parameter become very important. If (12) is taken literally, matter velocity is proportional to the impact parameter, and thus there is significant violation of special relativity in exceeding the velocity of light. It is much more reasonable to assume that the momentum density, instead of the matter velocity, is porportional to the impact parameter. If so, the important contribution to rotation parameters, in the limit $s \to \infty$, comes from hadronic matter moving at nearly the velocity of light. This situation is still not plausible.
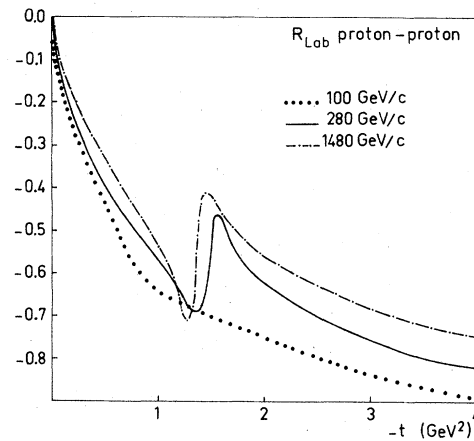
The simplest way to avoid this problem is to replace ω, the angular velocity for rigid rotation, by $\omega(b^2)$, a function of the impact parameter chosen such that

$$\omega(b^2) \to 0, \tag{23}$$

as $b^2 \to \infty$. In contrast to rigid rotation, such motion will be referred to as *soft rotation*.

This replacement of $\omega \to \omega(b^2)$ should be carried out for all the formulas of the last section. Thus, for example, Eq. (13) is now

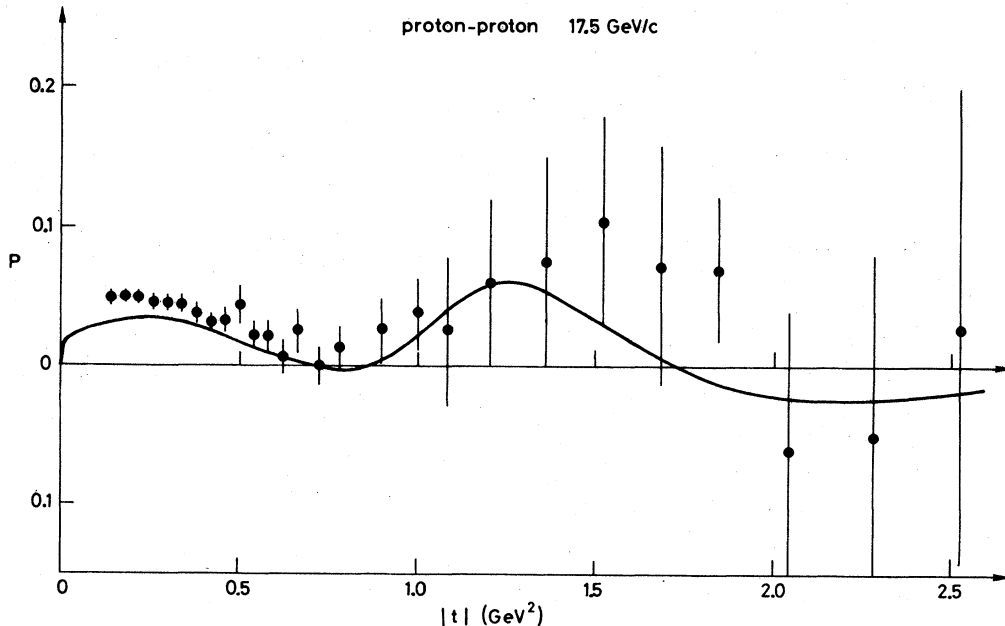$$S(s,b) = S_0(s) - \omega(b^2)\delta_x b S_1(s), \tag{24}$$

FIG. 14. Polarization at 17.5 GeV/c (data from Ref. 21). The curve is our soft-rotation model fit.
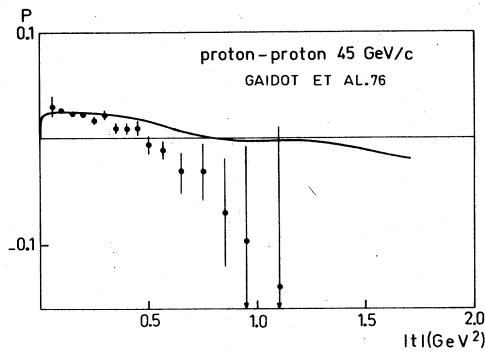
FIG. 15. Polarization at 45 GeV/c (data from Ref. 22). The curve is our soft-rotation model fit.

and the $F_s(\vec{b}^2)$ of (15) is given by

$$F_s(\vec{b}^2) = b\,\omega(b^2)F(\vec{b}^2). \tag{25}$$

Even though this generalization of introducing a function of the impact parameter is completely straightforward, we must be aware of the complications of this generalization. Rigid rotation has the following character. Consider a proton executing rigid rotation about the z axis, then for a given value of b_x the y component of the velocity is independent of b_y, and is given by (12). For soft rotation, this is no longer true. In other words, for soft rotation about the z axis, the y component of the velocity depends not only on b_x but also b_y. Therefore, in the impact-parameter representation, the effective energy of the colli-sion varies as the projectile passes through the target, and hence the s_{eff} of Eq. (10) has a spread.

We choose to ignore this complication for the present phenomenological analysis. The reason is that at present very little is known about had-ronic matter current, and that soft rotation is only meant to describe the gross features of this cur-rent. It thus seems reasonable to view s_{eff} as an average of the effective values of s as the projec-
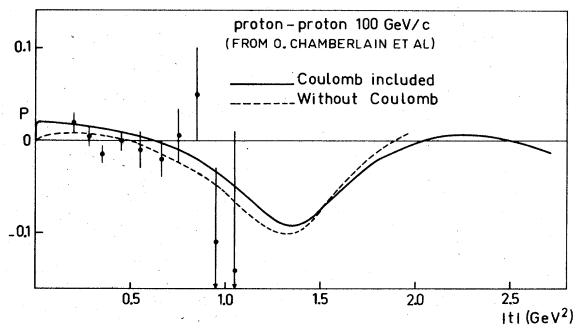

FIG. 16. Polarization at 100 GeV/c (data from Ref. 19). The solid curve is the fit of our soft-rotation model, and the dashed curve provides the result when the Coulomb contribution is not included.
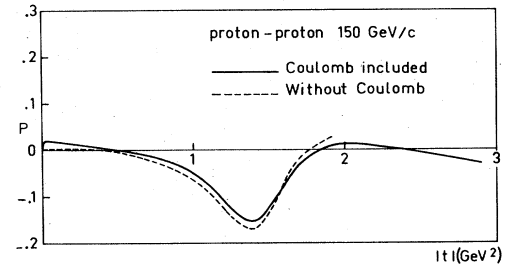

FIG. 17. The solid curve is our model prediction (soft rotation) for the polarization at 150 GeV/c, the dashed curve is the result when the Coulomb contribution is not included.

tile passes through the target, and v_y as an average value of the velocities for a given value of b_x. In the future, when hadronic matter current is better understood, it will be necessary to study such complications in detail, and it is likely that physi-cal effects may be directly measured.

VI. POLARIZATION AND R PARAMETER

We shall discuss the results in the two cases considered above.

A. Rigid rotation

The parametrization of the flip amplitude in-volves four parameters $\omega, C'_{\pm}, B$. The fit of the polarization data between 17–100 GeV/c shows that the value of the parameter ω in the Pomeron exchange is $\omega = -0.06$ GeV. The Regge flip para-meters are $C'_+ = 11.246$, $C'_- = -7.623$, $B = 1.942$ GeV^{-2}, and $\alpha(t)$ is the same as the nonflip. We present the results for the polarization at $p_{\text{lab}} = 100$ GeV/c compared with the data on Fig. 11. A pre-diction for P at $p_{\text{lab}} = 300$ GeV/c is given in Fig. 12 and shows large positive values in the dip re-gion. We have calculated the R parameter at dif-
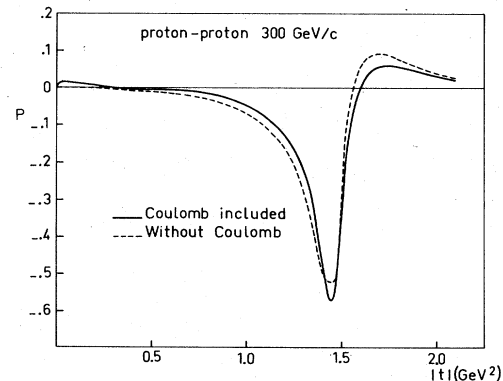

FIG. 18. The solid curve is our model prediction (soft rotation) for the polarization at 300 GeV/c, the dashed curve is the result when the Coulomb contribu-tion is not included.
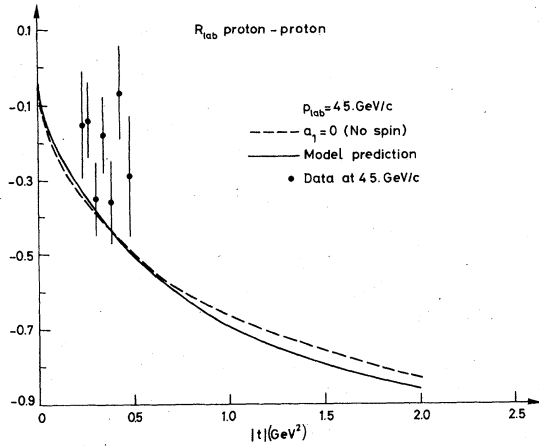
FIG. 19. R_{lab} at $p_{lab} = 45$ GeV/c (data from Ref. 23).
The solid curve is our soft-rotation model prediction.
The dashed curve is the prediction with no spin ($a_1 = 0$).

ferent energies 100, 280, and 1480 GeV/c shown
in Fig. 13.

The results on the R parameter have been re-
ported elsewhere.[20]

B. Soft rotation

Besides the condition (23), there is no guidance
in selecting the function $\omega(b^2)$. We choose, rather
arbitrarily, the Gaussian form

$$\omega(b^2) = \omega_0 e^{-b^2/b_0^2} , \tag{26}$$

where one additional parameter, b_0, has been in-
troduced. Another plausible form is

$$\omega(b^2) = \omega_0 \frac{b_0^2}{b^2 + b_0^2} . \tag{27}$$

With (26), we have five parameters in that case
whose values are $\omega_0 = -0.06$ GeV, $b_0 = 3.75$ GeV^{-1}.
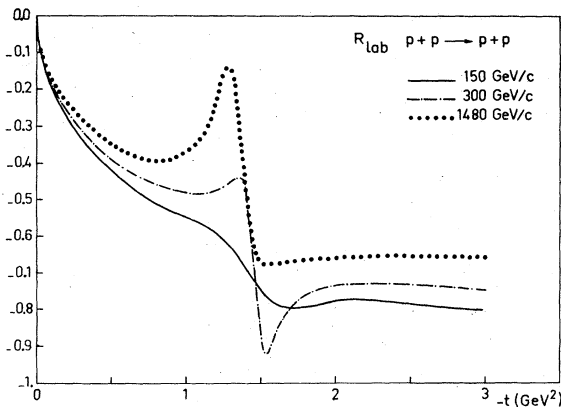The Regge flip parameters are $C_+' = 3.547$, C_-'

FIG. 20. Predictions of R_{lab} at 150, 300, 1480 GeV/c
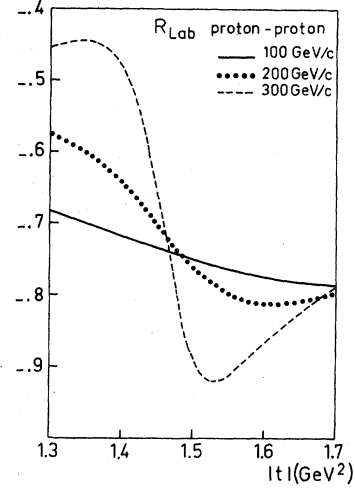(soft rotation).

FIG. 21. Predictions of R_{lab} at 100, 200, 300 GeV/c
for $1.3 < |t| < 1.7$ GeV^2 (soft rotation).

$= -1.538$, $B = 0.597$ GeV^{-2}. With these parameters
the profile function $F_s(\vec{b}^2)$ which corresponds to
the spin-dependent part of the Pomeron is plotted
in Fig. 2 and as expected it exhibits a peripheral
behavior.

The results on the polarization are in Figs. 14,
15, 16 for the energies 17.5, 45, and 100 GeV/c,
there is a reasonable agreement with experiments
in particular at low t values. We also present on
Figs. 17 and 18 predictions of our model for p_{lab}
$= 150$ and 300 GeV/c which will be soon compared
with new experimental data.

A detailed analysis of the amplitudes in the
soft-rotation case shows that the real part of the
flip amplitude a_1 is positive for small t values
and has a zero at $|t| \simeq 1.1$ GeV^2 at $p_{lab} = 17.5$
GeV/c which moves in when the energy increases.
As a result the double zero of the polarization at
17.5 GeV/c gives rise to a single zero for smaller
and smaller t values when s increases. For
$|t| < 1$ GeV^2 the main contribution of the polar-
ization comes from Ima_0 Rea_1 [see Eq. (20)], and
this is the reason why P becomes negative in this
t range at high energies. The imaginary part of
the nonflip amplitude a_0 has a zero which also
moves in when s increases, and at $p_{lab} = 300$ GeV/c
it occurs at the dip position $|t| \simeq 1.3$ GeV^2. This
gives for P a maximum negative value larger and
larger when Rea_0 decreases as the energy
increases.

We have calculated the R parameter at different
energies: 45, 100, 280, and 1480 GeV/c in Figs.
19–21. In order to emphasize the influence of a_1,
on R_{lab} we plotted at 45 GeV/c a curve with no
spin dependence ($a_1 = 0$). We observe that at low
t ($-t < 0.5$ GeV^2) the spin effect is negligible,

while for $-t \sim 1$ GeV^2 the two curves separate.
The existing data at low t[23] have too large errors
and so yield no precise conclusion. From our re-
sult, future experiments at large $-t$ will be of in-
terest for the detection of spin effect if reasonable
errors are obtained. At Fermilab or CERN SPS
energies, the R parameter develops a rapid vari-
ation between 100 and 300 GeV/c around $-t = 1.3$
GeV^2 at the position of the dip in the differential
cross section (see Fig. 21). This effect can be
detected, because we notice in Eq. (20), that if
no spin effect was present R would behave as
$\cos(\theta - \theta_R)$, so any departure from that curve in-
dicates the presence of spin interference. Let us
stress that for the energies above 200 GeV/c
where the Regge background becomes negligible,
the predictions of our model for the Pomeron spin
amplitude depend on two parameters ω_0 and b_0 for
the case of soft rotation.

VI. CONCLUSION

We have presented a phenomenological analysis
of pp elastic scattering from $p_{\text{lab}} = 14$ GeV/c up to
2000 GeV/c by means of a new impact picture
with a specific spin dependence. The model de-
rived from the asymptotic energy behavior of
relativistic quantum field theory gives a fair de-
scription of the data in particular at ISR energies
and large momentum transfers. It shows that no
significant modifications on our ideas on diffrac-
tion are necessary and contradicts the statement
according to which eikonal models are inadequate
for high-energy processes.[24] The absence of a
second dip at ISR energies[25] is due to the follow-
ing facts: (i) The energy dependence of the Pom-
eron is described by a complex function of energy
$S(s)$, (ii) the profile function $F(\vec{b}^2)$ is close to the
unitarity limit near $b \sim 0$, and for large b decrea-
ses less rapidly than a Gaussian. This flattening
of $F(\vec{b}^2)$ at small b is produced by a zero at $|t| \sim 5$
GeV^2 in $\tilde{F}(t)$.

Once the phenomenologically satisfactory im-
pact picture of Sec. II is available, it is then pos-
sible to study the spin dependence at high energies
by combining the impact picture with the hadronic
matter current of Chou and Yang.[8] Two of the
simple possibilities are the cases of rigid rotation

and soft rotation. While rigid rotation is the sim-
plest in the sense of involving the least number of
parameters, it has serious theoretical difficulties
in the limit of infinite energy. Soft rotation, on
the other hand, involves at least one more para-
meter but seems to have no conceptual difficulty.

For the two phenomenological models of rigid
rotation and soft rotation, the predictions for both
polarization and the R parameter are quite differ-
ent. This means that these two models can be
easily differentiated experimentally by measuring
either the polarization or the R parameter. In
view of the theoretical difficulty with the case of
rigid rotation, we prefer the model of soft ro-
tation. Whether this prejudice of ours is justified
or not can probably be determined by experiments
in the near future.

We have discussed in this paper on the case of
proton-proton scattering. The ideas and the an-
alysis can clearly be applied to many other two-
body elastic scattering processes. In particular,
recent measurements[26] show that the Λ-proton
polarization is larger than the proton-proton po-
larization which might indicate that the matter in-
side a Λ rotates faster than in the case of a pro-
ton. In this connection, we mention our specu-
lation about a possible connection between the
angular velocity of rotation and the isoscalar mag-
netic moment.[20]

In conclusion, we reiterate that the measure-
ment of the R parameter at Fermilab or CERN
SPS will be an important test on the validity of
the different pictures of the matter motion inside
a proton, because several distinct theoretical
predictions are now available.

---

*Postal address: CNRS-Luminy-Case 907, Centre de
Physique Théorique, F-13288 Marseille Cedex 2,
France.
†On leave from Harvard University, Cambridge, Mass-
achusetts 02138.
[1]H. Cheng and T. T. Wu, Phys. Rev. D **1**, 2775 (1970);

Phys. Rev. Lett. **24**, 1456 (1970).
[2]M. Froissart, Phys. Rev. **123**, 1053 (1961). A. Martin,
Phys. Rev. **129**, 1432 (1963); Nuovo Cimento **42**, 930
(1966).
[3]U. Amaldi et al., Phys. Lett. **44B**, 112 (1973); S. Amen-
dolia et al., ibid. **44B**, 119 (1973).

[4]H. Cheng, J. Walker, and T. T. Wu, Phys. Lett. 44B, 97 (1973); H. Cheng and T. T. Wu, in *High Energy Collisions—1973*, proceedings of the Fifth International Conference, Stony Brook, edited by C. Quigg (AIP, New York, 1973).

[5]T. T. Wu, in *Proceedings of the XVIIIth International Conference on High Energy Physics, Tbilisi, 1976*, edited by N. N. Bogolubov *et al.* (JINR, Dubna, 1977), Vol. I, p. A5-23.

[6]T. T. Wu and C. N. Yang, Phys. Rev. 137, B708 (1965).

[7]T. Chou and C. N. Yang, Phys. Rev. 170, 1591 (1968); 175, 1832 (1968); Phys. Rev. Lett. 20, 1213 (1968).

[8]T. Chou and C. N. Yang, Nucl. Phys. B107, 1 (1976).

[9]H. Cheng and T. T. Wu, Phys. Rev. 184, 1868 (1969).

[10]P. Kirk *et al.*, Phys. Rev. D 8, 63 (1973).

[11]J. Allaby *et al.*, Phys. Lett. 30B, 500 (1969); U. Amaldi *et al.*, *ibid.* 44B, 112 (1973); 62B, 460 (1976); A. Carroll *et al.*, *ibid.* 61B, 303 (1976); S. Denisov *et al.*, *ibid.* 36B, 415 (1971); 36B, 529 (1971); K. Foley *et al.*, Phys. Rev. Lett. 19, 857 (1967).

[12]U. Amaldi *et al.*, Phys. Lett. 43B, 231 (1973); 66B, 390 (1977); V. Bartenev *et al.*, Phys. Rev. Lett. 31, 1367 (1973); G. Belletini *et al.*, Phys. Lett. 14, 164 (1965); G. Beznogikh *et al.*, *ibid.* 39B, 411 (1972).

[13]J. Allaby *et al.*, Phys. Lett. 25B, 156 (1967); 34B, 431 (1971); Nucl. Phys. B52, 316 (1973).

[14]N. Kwak *et al.*, Phys. Lett. 58B, 233 (1975); H. de

Kerret *et al.*, *ibid.* 62B, 363 (1976); 68B, 374 (1977); J. L. Hartmann *et al.*, Phys. Rev. Lett. 39, 975 (1977).

[15]L. Van Hove, Nucl. Phys. B122, 525 (1977).

[16]C. Bourrely, A. Martin, J. Soffer, and D. Wray, J. Phys. G 3, 295 (1977).

[17]T. Chou and C. N. Yang, Phys. Rev. D 17, 1889 (1978).

[18]C. Bourrely and J. Soffer, Lett. Nuovo Cimento 19, 569 (1977).

[19]R. Kline *et al.*, in *High Energy Physics with Polarized Beams and Targets*, proceedings of the Argonne Symposium, 1976, edited by M. L. Marshak (AIP, New York, 1976).

[20]C. Bourrely, J. Soffer, and T. T. Wu, Phys. Lett. 76B, 481 (1978).

[21]M. Borghini *et al.*, Phys. Lett. 31B, 405 (1970), 36B, 501 (1971).

[22]A. Gaidot *et al.*, Phys. Lett. 61B, 103 (1976).

[23]J. Pierrard *et al.*, Phys. Lett. 61B, 107 (1976).

[24]U. Sukhatme, Phys. Rev. Lett. 38, 124 (1977).

[25]The effect of inelastic diffraction can be used to fill in the second dip; see P. Crozier and B. Webber, Nucl. Phys. B115, 509 (1976); Phys. Rev. D 18, 334 (1978); R. Henzi and P. Valin, in *Proceedings of the 1977 European Conference on Particle Physics, Budapest*, edited by L. Jenik and I. Montvay (CRIP, Budapest, 1978).

[26]B. Edelman *et al.*, Phys. Rev. Lett. 40, 491 (1978).